Solar Phys (2020) 295:161
https://doi.org/10.1007/s11207-020-01731-y

# The Evolution of Coronal Holes over Three Solar Cycles Using the McIntosh Archive

**Ian M. Hewins[1] · Sarah E. Gibson[2] · David F. Webb[1] · Robert H. McFadden[1] · Thomas A. Kuchar[1] · Barbara A. Emery[1,2] · Scott W. McIntosh[2]**

Received: 23 April 2020 / Accepted: 31 October 2020


**Abstract** Using the McIntosh Archive of solar features, we analyze the evolution of coronal holes over more than three solar cycles. We demonstrate that coronal-hole positions and lifetimes change significantly on time scales from months to years, and that the pattern of these changes is clearly linked to the solar-activity cycle. We demonstrate that the lifetimes of low-latitude coronal holes are usually less than one rotation but may extend to almost three years. When plotted over time, the positions of low-latitude coronal holes that remain visible for over one rotation track the sunspot butterfly diagram in terms of their positions on the Sun over a solar cycle. Finally, we confirm that coronal holes do not in general rigidly rotate.

**Keywords** Coronal holes - solar cycle · Observations - sunspots · Magnetic fields

✉ I.M. Hewins
imh.68ont@gmail.com

S.E. Gibson
sgibson@ucar.edu

D.F. Webb
david.webb@bc.edu

R.H. McFadden
crmcfadden11@gmail.com

T.A. Kuchar
thomas.kuchar@bc.edu

B.A. Emery
barbara.emerygeiger@gmail.com

S.W. McIntosh
mscott@ucar.edu

1 Institute for Scientific Research, Boston College, Chestnut Hill, MA, USA

2 High Altitude Observatory, National Center for Atmospheric Research, Boulder, CO, USA

Published online: 13 November 2020

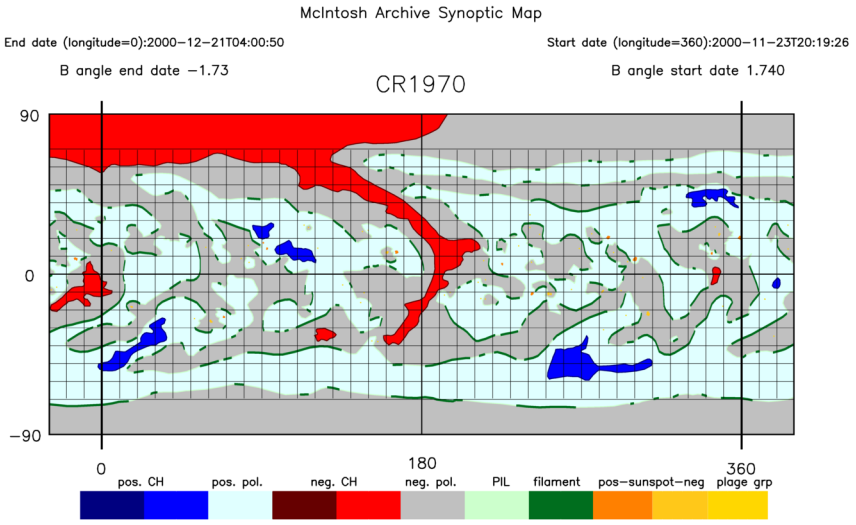


**Figure 1** The McIntosh Archive (McA) synoptic maps are a global representation of the evolving solar magnetic field. Each map covers 360° of a Carrington rotation. The extra 30° on either side overlaps with the previous and following maps. Magnetic features are identified by a distinct color: Blue represents positive-polarity coronal holes, red represents negative coronal holes, pale blue represents areas of dominant positive polarity, gray represents areas of dominant negative polarity, dark green represents filaments, light green represents polarity inversion lines, dark orange represents positive polarity sunspots, light orange represents negative polarity sunspots and (small) yellow spots represent plage regions. The full archive is publicly available at www2.hao.ucar.edu/mcintosh-archive/four-cycles-solar-synoptic-maps.

## 1. Introduction

In 1964 (the beginning of Solar Cycle 20), Patrick McIntosh began creating hand-drawn synoptic maps of solar magnetic features, based on H$\alpha$ images (Figure 1). Using magnetograms, he included magnetic polarity inversion lines that connected filaments separated by many degrees, thus establishing the polarity of other features such as sunspots and plage and revealing the large-scale organization of the solar magnetic field (McIntosh, 1979). Coronal holes were eventually included using ground-based He 10830 Å images from the National Solar Observatory (NSO) Kitt Peak starting in 1981 and later (after 1992) from NSO's Sacramento Peak. Note, McIntosh also used He 10830 Å data to map coronal holes in 1978, but only for three rotations.

In this article, we make use of the McIntosh Archive (McA: Webb et al., 2018), and we augment it by filling in missing maps and applying McIntosh's method to add coronal-hole data to the maps of rotations prior to 1981 using He 10830 Å observations from Kitt Peak. The term "coronal hole" is used to denote the darkest areas on the solar surface, typically as measured in ultraviolet and X-ray radiation, and also the lowest-intensity regions measured above the solar limb, such as during total solar eclipses. Coronal holes are regions of low density and temperature plasma on the solar disk with magnetic fields that open or extend into the heliosphere (Cranmer, 2009). The sizes and evolution of coronal holes vary with the solar-activity cycle. Around minimum solar activity the Sun's dominant magnetic-field component is a rotationally aligned dipole, so large coronal holes cover the polar caps of the Sun. During solar maximum only small mid-latitude holes exist and they have shorter lifetimes. During the rising and declining phases of a solar cycle, coronal holes can exist at

any latitude and can evolve into elongated structures stretching equatorward from the Pole (Zirker, 1977; Harvey and Recely, 2002). Figure 1 shows an example of such an elongated polar coronal-hole extension crossing the Equator.

The concept that coronal holes involve regions of open magnetic field that expand into interplanetary space was recognized after the first in-situ solar-wind observations utilized X-ray sounding rocket images to identify a large coronal hole as the solar source of a strong high-speed stream as measured by spacecraft (Wilcox, 1968; Hundhausen, 1972; Krieger, Timothy, and Roelof, 1973). Coronal holes and high-speed wind streams were also linked to approximately 10% of geomagnetic storms seen at 1 AU (Zhang et al., 2007). The properties of high-speed solar-wind streams depend on the geometry of open field lines (Wang and Sheeley, 1990) that are associated with coronal holes.

Webb et al. (2018) show that over at least Solar Cycles 21 – 23, the McA maps highlight the diverging behavior of what appear to be two populations of coronal holes: high-latitude coronal holes that move poleward to cover the poles and low-latitude coronal holes that move equatorward and track the sunspot butterfly pattern. Overlaying plots of coronal-hole evolution with plots of zonal flows (torsional oscillations) associated with the migration of the near-surface magnetic field (Howe, 2009) demonstrates that the coronal-hole locations match well with the poleward and equatorward magnetic flows.

Waldmeier (1957, 1981) first studied the evolution of high-latitude and polar coronal holes over four solar cycles using coronal green-line data. Later studies showed that these large-scale rearrangements of the open flux in unipolar areas led to the polar-field reversals around solar-cycle maximum and the subsequent reformation of the polar coronal holes (Hundhausen, Hansen, and Hansen, 1981; Webb, Davis, and McIntosh, 1984; Harvey and Recely, 2002). More recently Golbeva and Mordvinov (2017) studied these rearrangements of magnetic flux and formation of polar coronal holes in Solar Cycles 23 and 24. They found that during these solar cycles, "ensembles of coronal holes" appeared within unipolar magnetic regions associated with decaying activity complexes. Thus, particularly in Solar Cycle 24, the decay of large activity regions in the South led to formation of an extensive coronal-hole ensemble, which in turn became the southern polar coronal hole.

Other recent studies of coronal-hole evolution have used SDO (*Solar Dynamics Observatory*) AIA (*Atmospheric Imaging Assembly*) and HMI (*Helioseismic and Magnetic Imager*) data to analyze Solar Cycle 24 coronal-hole structure and evolution. In particular, Heinemann et al. (2018) studied the evolution of one coronal hole over 360° solar rotations, finding that the growth phases matched the in-situ solar-wind speeds. Heinemann et al. (2020) measured the rates of change of 16 coronal-hole areas and their magnetic fields. Hofmeister et al. (2017, 2019) analyzed the intensities and magnetic structure and fluxes of many low-latitude coronal holes over several years.

The large-scale motions of solar surface features including coronal holes must somehow be related to the internal fluid dynamics of the Sun, and must be accounted for in dynamo models. Generally these observations agree with flux-transport dynamo models (Karak et al., 2014), and with numerical models of the evolution of photospheric magnetic fields (Devore et al., 1985; Jiang et al., 2014). However, the general patterns of coronal-hole evolution and how they migrate over a solar cycle are not well studied or understood.

In this article we use the McA synoptic maps to study the evolution of coronal holes over more than three consecutive solar cycles, focusing on the lifetimes of the coronal holes. In Section 2 we briefly review the McIntosh Archive. In Section 3 we present our methodology for tracking coronal holes. In Section 4 we present the results of our solar-cycle analysis of coronal holes. In Section 5 we consider the issue of differential rotation, and in Section 6 we present our conclusions.

## 2. The Augmented McIntosh Archive

Patrick McIntosh and his assistants produced these synoptic maps, with some gaps, from 1964 into 2009. R.H. McFadden and I.M. Hewins were McIntosh's last assistants. McFadden was trained by McIntosh to make the original hand-made maps and Hewins was trained by McIntosh to digitize the original maps with Photoshop. McFadden later trained Hewins to make original maps in order to assist with the augmentation. Each map represents a 360° Carrington rotation. The result was a record of 45 years, 600 Carrington rotations, or over four solar cycles of synoptic maps. These hand-drawn synoptic maps initially combined the data from H$\alpha$ images with magnetograms. Polarity inversion lines were estimated from the magnetograms and confirmed by filament positions when the data were combined. Coronal-hole boundaries were later included in the maps taken from ground-based He 10830 Å images from NSO's Kitt Peak and eventually Sacramento Peak observatories. McIntosh's map-making methodology, and the digitization and archiving of these maps, are described in further detail by Webb et al. (2018). The resulting maps are publicly available at NOAA's National Centers for Environmental Information (Figure 1).

We have digitized all 600 Carrington rotations including an augmentation in which, using McIntosh's methodology, we have produced any missing or incomplete maps. In particular, 82 maps (mostly in Solar Cycle 21) had coronal holes added as part of the current augmentation effort using the coronal-hole data that became available starting in July 1974 when Kitt Peak began producing He 10830 Å images.

The analysis presented in this article thus incorporates the longest (to our knowledge) consecutive searchable coronal-hole database generated to date. The McIntosh archive's strength is that it is ideally suited for a combined analysis of different solar magnetic features, including sunspots, plages, filaments, and coronal holes. By looking at how different features appear in relation to each other over numerous solar cycles, we can examine connected patterns that exist within and between solar cycles. In particular, we are interested in coronal-hole positions and lifetimes as a function of solar-cycle phase.

## 3. Coronal Hole Tracking Methodology

The McIntosh archive consists of FITS-formatted files in which every pixel in latitude and longitude has a unique numerical value that identifies the magnetic feature present at that location (see Figure 1). In order to track the lifetimes of coronal holes from map to map over consecutive Carrington rotations, we extract the locations of all regions defined as coronal holes and separate them by polarity (negative or positive). We are aware of the limitations and difficulties involved in accurately identifying coronal-hole boundaries. When McIntosh began, He 10830A was the only consistently available source for coronal-hole data. McIntosh developed a technique that is simple, easy to reproduce, and objective. All cartographers were trained and tested for consistency before their work was included as a final product. He 10830 Å data from NSO observatories were used almost exclusively throughout the study. To limit projection effects, data were limited to within 30° of the central meridian using images taken every four to five days.

Coronal holes were identified in the digitized maps using IDL's contour.pro procedure. This allows us to establish the coronal holes' maximum and minimum latitudes and longitudes, along with their centroid position (latitude, longitude) and area (degrees squared, and adjusted for projection effects, mapping from rectangular Cartesian coordinates to spherical coordinates). An analysis of coronal-hole area is beyond the scope of the current article,

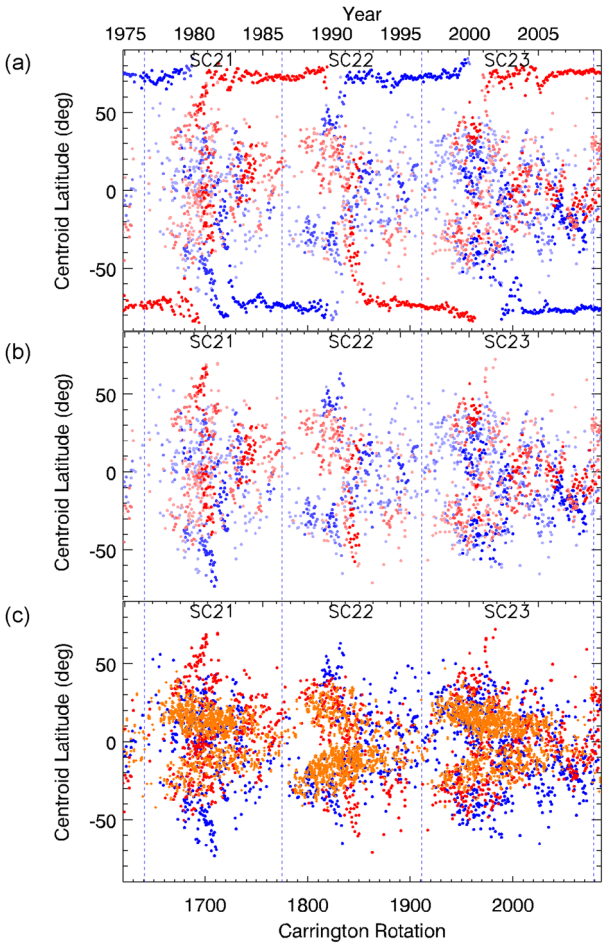


**Figure 2** Coronal-hole centroid latitude vs. Carrington Rotation (bottom) and year (top) for over three solar cycles (roughly Solar Cycles 21 – 23). Red represents negative polarity and blue represents positive polarity. The beginning of the solar cycles are marked with a vertical dashed line. (**a**) All coronal holes with darker shades representing longer lifetimes; (**b**) Only long-lived, low-latitude coronal holes, with the darker shades representing longer lifetimes, i.e. the number of rotations a given coronal hole or grouping of coronal holes recurs; (**c**) Long-lived low-latitude coronal holes and sunspots (orange).

however Mazumder, Bhowmik, and Nandy (2018) have published a study that includes plots of the evolution of coronal-hole areas (in $Mm^2$) over Solar Cycles 21 – 23 using an earlier (less complete) version of the McIntosh archive.

The full extent of polar coronal holes can be difficult to observe because of projection effects and the annual B-angle tilt variation which alternately obscures North and South Poles. In the case of well-established polar holes, we generally infer an extension to $\pm 90^\circ$ helio-latitude. We note that polar coronal-hole centroids are extremely difficult to calculate due to both projection effects and the fact that we can only see one face of the Sun at a time (so the full span of the polar coronal hole is not observed co-temporally). Therefore, rather than attempt to determine the centroid in polar coordinates, the centroid positions plotted for polar coronal holes in Figure 2a are a representation of the average distance between the Pole and the most equatorward extents of the polar coronal hole as a function of longitude. This creates a more accurate visual representation of the positions of the polar coronal-hole boundaries in relation to the more poleward of the low-latitude coronal-hole populations.

Using the maximum and minimum longitudes and latitudes to compare the positions of coronal holes from one rotation to the next, we determine if there is any overlap of the coordinates of a coronal hole of a given polarity from one Carrington rotation to the next. If

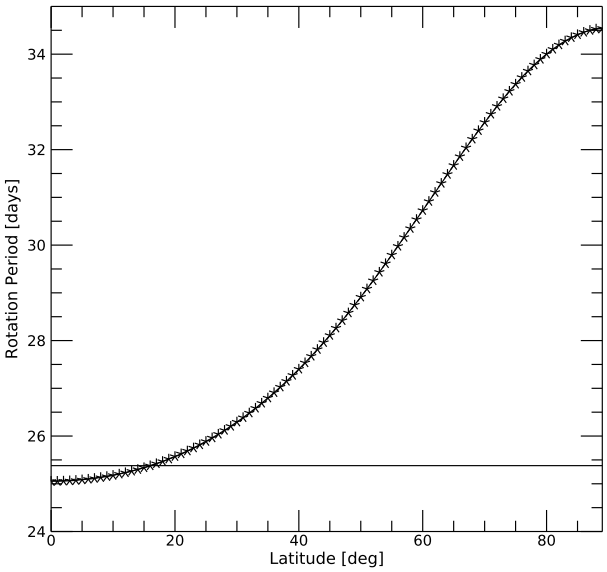


**Figure 3** Solar-surface rotation rates used in this article. Solid line represents the rigid sidereal rotation rate of 25.4 days, the so-called "Carrington" rate. The asterisks show the differentially rotating photospheric rate as determined by tracking magnetic features (Snodgrass, 1983). Note the latitude where the curves cross the horizontal solid line (approximately 20°) will rotate at the Carrington rate, while latitudes above this will appear to rotate retrograde (slower) and below this will appear to rotate somewhat prograde (faster). Also note that in the rest of the article we apply rigid rotation at the synodic rotation rate of 27.3 days since the McIntosh Archive maps are observed from the Earth's frame of reference.

so, we identify it as the same coronal hole, and we update the latitude–longitude bounding box for that identified coronal hole to represent the values of the later Carrington rotation. This is our baseline, "solid rotation" case where we assume coronal holes at all latitudes rotate at the Carrington rate (Figure 3, horizontal solid line; see Section 5 for a discussion of the effects of differential rotation). By tracking coronal holes in this manner, we establish a total lifetime, or number of Carrington rotations, that they persist.

We subdivide the resulting tracked set of legacy coronal holes into three primary varieties: polar, short-lived low-latitude, and long-lived low-latitude. We define "short-lived" as only appearing on one Carrington rotation and "long-lived" as appearing in approximately the same location on more than one consecutive Carrington rotation. For the purposes of this study, we define "low-latitude" as those coronal holes that do not reach $\pm 90^\circ$ helio-latitude at any longitude of a given Carrington rotation. This is done to simplify the analysis. In fact, some of the coronal holes that we call low-latitude are part of a population that ultimately forms the polar hole (Webb et al., 2018). Indeed, Figure 2 shows a pattern similar to the "rush to the poles" also seen with filaments (Altrock, 1997). Moreover, at times a polar coronal hole has an extension that reaches low latitudes, and in such cases we label them still as polar holes because they are part of a larger entity that covers the poles (see Figure 1). These polar extensions can be significant contributors to Earth-intersecting solar wind (Gibson et al., 2011).

For cases in which a coronal hole splits into more than one smaller coronal hole overlapping the original bounding box, or conversely where multiple coronal holes merge into a larger coronal hole in a subsequent Carrington rotation, we identify all of the smaller coronal holes as part of the same "legacy" coronal hole with a shared lifetime. The exception

is for cases where a low-latitude coronal hole or grouping of coronal holes merges with a pre-existing polar coronal hole. In such cases, the lifetime of the legacy low-latitude coronal hole is considered to end. This can result in an underestimate of low-latitude coronal-hole lifetimes. In particular, we note that the extension from the northern polar hole seen in Figure 1 was a short-lived (single Carrington rotation) phenomenon, such that the grouping of low-latitude coronal holes that formed it actually reappeared in the following Carrington rotation, at which point they were considered a new legacy coronal hole and their lifetime count reset.

## 4. Coronal Holes and the Solar Cycle

We tracked a total of 1070 low-latitude coronal holes from November 1974 to August 2009, or roughly 35 years. Of those 1070 low-latitude coronal holes, 729 or 68% were visible on only one rotation. 341 or 32% lasted two or more rotations. Of that 32% that was visible in two or more rotations, 46% or 157 appeared only on two rotations. Although the majority of low-latitude holes were fairly short-lived, a notable set did last many rotations. 21 or 2% of all low-latitude coronal holes lasted longer than ten rotations. Only four, or 0.4%, of all low-latitude coronal holes lasted longer than 20 rotations.

When all coronal holes are plotted by latitude and Carrington rotation over three solar cycles (assuming a rigid 27.3 day synodic rotation rate), a clear pattern is evident that follows the 22-year solar magnetic cycle (Figure 2). In this figure, the beginning of the solar cycles are marked with a vertical dashed line and are based on Sunspot Index and Long-term Solar Observations (SILSO) sunspot numbers (Version 2 SILSO data available from The Royal Observatory of Belgium, Brussels at www.sidc.be/silso/).

The change in polarity for polar coronal holes is a process that takes close to two years and occurs roughly six months earlier in the North Pole than in the South Pole for all three cycles that we have examined (Lowder, Qiu, and Leamon, 2017; Webb et al., 2018). Thus, there is a period when the North Pole has reversed polarity but the South has not yet reversed, resulting in the same polarity dominating both poles for a period of about six months. Note that this occurs at a time when there are no well-formed polar coronal holes and so is not evident in our figures.

During the polar magnetic-field reversal period, a set of long-lived coronal holes with the opposite polarity appear at increasingly more poleward latitudes, in a manner reminiscent of the "rush to the poles", of polar-crown filaments (Lockyer, 1931; Altrock, 1997), which has also been observed in the McIntosh archive (Webb et al., 2018).

For the few months while the polarity reversal is happening, there are no polar coronal holes at all, or a coronal hole makes it to the pole briefly before disappearing again. This time period is essentially solar sunspot maximum. Eventually, the ascending/descending branch of coronal holes reach latitudes of about $\pm 70^{\circ}$, and the new-polarity polar coronal holes are established. Approximately four to five years after maximum, the polar coronal holes may create extensions that eventually break off and become low-latitude coronal holes. This is visible in Figure 2a as a slight equatorward shift of the polar coronal-hole centroid latitudes, followed by the appearance of non-polar coronal holes at somewhat lower latitudes, particularly visible just before Solar Cycle 22 maximum.

When we look only at long-lived, low-latitude coronal holes (Figure 2b) we see a pattern reminiscent of the sunspot butterfly diagram. The main departure from the classic sunspot butterfly pattern is the ascending/descending branches of long-lived non-polar coronal holes already commented on. However, Figure 2c demonstrates how the other low-latitude coronal

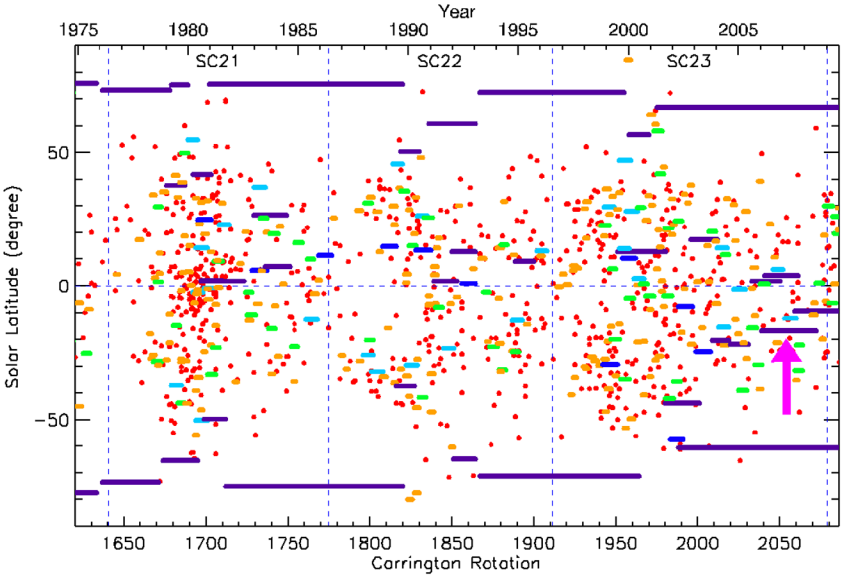


**Figure 4** Similar to Figure 2a, however, in this plot long-lived coronal holes (both polar and low-latitude) are plotted as a straight line originating at the centroid of the coronal hole's first appearance. Thus, in this plot both color and extension to the right indicates lifetimes of coronal holes. As in previous figures, coronal-hole tracking assumes a rigid 27.3 day rotation rate. Red represents coronal holes lasting only one rotation, yellow 2 – 3, orange 4 – 5, green 6 – 7, cyan 8 – 9, blue 10 – 11, and purple 12+. The long-lived coronal-hole pattern shown in Figure 6 is indicated with an arrow. A similar plot for Solar Cycle 24 was created by Krista, McIntosh, and Leamon (2018). Note the polar coronal holes in purple, their gaps, and the lower latitude purple band showing a lower centroid for the long-lived coronal holes around solar maximum. The beginning of each solar cycle (minimum smoothed sunspot number) is marked with a vertical dashed line.

holes appear at decreasing latitudes as the solar cycle progresses in a manner similar to the sunspots. Both coronal holes and sunspots follow a butterfly pattern, although coronal holes also have a poleward branch during the ascending phase (see also McIntosh et al., 2015; Gibson et al., 2017). In some cases, the proximity of the centroid to the Equator indicates a trans-equatorial coronal hole that can last a year or more despite shear forces present across the Equator associated with differential rotation (see Section 5).

Figure 4 further illustrates the lifetimes of coronal holes. We see that polar coronal holes tend to last many years, but there are also low-latitude, long-lived coronal holes that persist for more than a year (purple). Nevertheless, the majority are red dots, i.e. low-latitude coronal holes that appear on only one Carrington rotation. The number of each type of legacy coronal hole and their lifetimes can also be seen in Figure 5.

As discussed in Section 3, low-latitude coronal holes sometimes evolve into a pattern of more than one smaller coronal hole that together span the region of the original coronal hole. The converse is also sometimes true, where a few smaller coronal holes appear to have joined together to form a larger one on the next rotation. Whether this represents a true evolution of magnetic structure or whether other factors affecting coronal-hole visibility may have impacted our ability to identify an open magnetic region as a single coherent coronal hole is not clear. However, our practice has been to treat the collected region as one in tracking lifetimes. In one particularly interesting case, a set of coronal holes manifested as an evolving pattern over a period of 37 rotations (Figure 6) at times demonstrating both

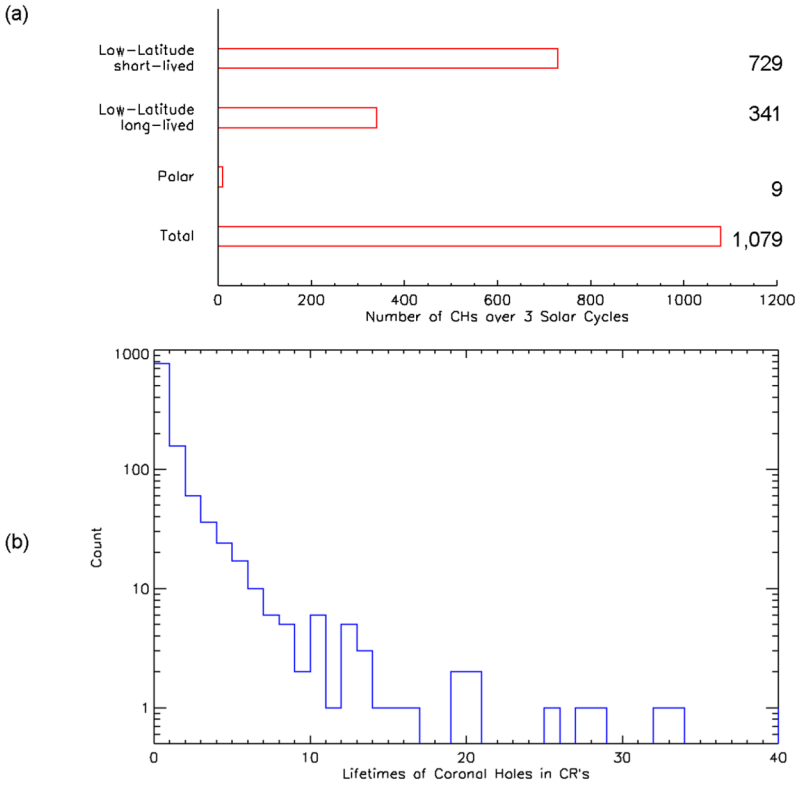


**Figure 5** (**a**) Number of coronal holes by type (see Section 3) for assumed rigid 27.3 day rotation. The total numbers counted are equivalent to the total numbers of colored dots/lines in Figure 4 – thus, representing the number of legacy coronal holes (see Section 3). (**b**) Logarithmic histogram of low-latitude coronal–hole lifetimes. Single-rotation lifetimes, i.e. short-lived low-latitude coronal holes, dominate. The long-lived, low-latitude coronal holes have a distribution of lifetimes, including a few that persist for more than a year.

prograde and retrograde motion in a manner that may arise from the evolution of centroid latitude over time.

## 5. Differential Rotation of Coronal Holes

Figure 6 shows a "stack" plot showing how equatorial coronal holes shift in longitude as a function of time, illustrating that long-lived, low-latitude coronal holes are not rotating rigidly. If they were, their centroid longitude would be constant from rotation to rotation, and they would appear as a vertical pattern in the stack plot. The rightward slant is consistent with a rotation that is prograde (faster) with respect to the Carrington rate of 27.3 days, which is the rate expected at mid-latitudes for photospheric flows.

Figures 7, 8, 9 show that prograde rotation at low (equatorial) latitudes occurs for all three solar cycles studied, and that retrograde (slower) rotation is evident at higher latitudes (see also Gibson et al., 2017). This is akin to the differential rotation at the photosphere (Figure 3) in that it implies that the Equator is moving faster than the Poles. However, the situation is more complex for coronal holes as the slopes of the features seen in Figures 7 – 9

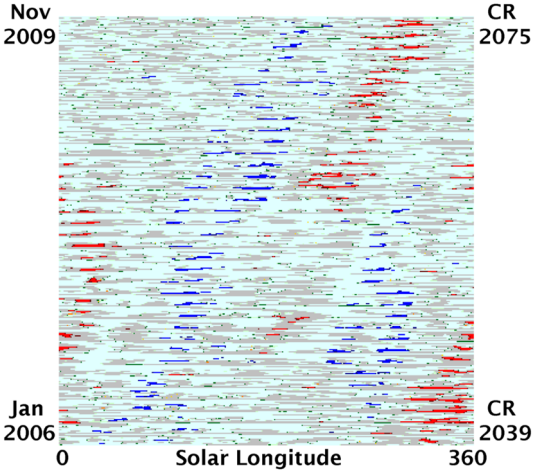


**Figure 6** "Stack" plot illustrating the continued existence of one low-latitude coronal-hole group for over 37 rotations or almost three years (Carrington rotations 2039 – 2075). Horizontal axis is longitude; a sequence of equatorial slices (-25° to 55° in latitude) is stacked along the vertical axis with time increasing from bottom to top. This range in latitudes was chosen to capture the full evolution of the coronal-hole centroids for the full time interval shown. Colors represent magnetic features as in Figure 1. Blue represents positive polarity coronal holes, red represents negative coronal holes, pale blue represents areas of dominant positive polarity, gray represents areas of dominant negative polarity, dark green represents filaments, light green represents polarity inversion lines, orange represents sunspots, and (small) yellow spots represent plage regions. The positive-polarity coronal hole is blue and begins in the lower left of the stack plot. The coronal hole divides and recombines over time, but the presence of a legacy group of coronal holes clearly persists for all 37 rotations. The slope of the feature generally exhibits a prograde (faster) motion relative to the Carrington rotation rate, as expected for this equatorial latitude range based on observed photospheric differential rotation rates (see Figure 3).

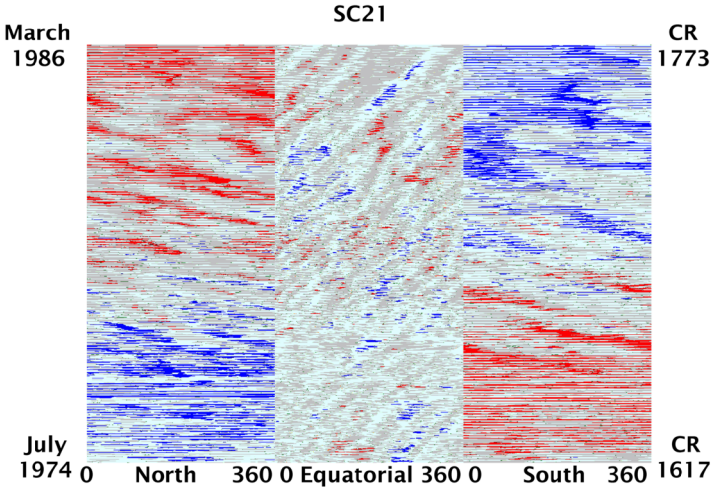


**Figure 7** "Stack" plots as in Figure 6 for different latitude range for Solar Cycle 21. Horizontal axis is longitude; a sequence of slices is stacked along the vertical axis with time increasing from bottom to top. Including all of the (left) north polar zone (30° to 70° latitude), (middle) equatorial zone (-20° to +20° latitude), and (right) south polar zone (-70° to -30° latitude).

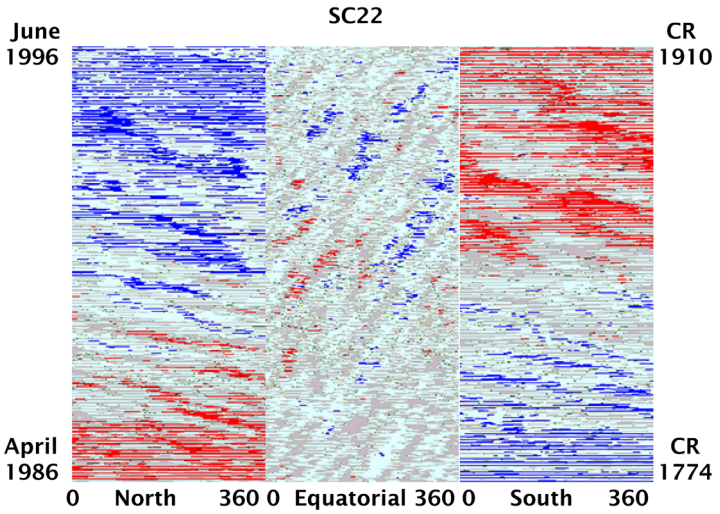


**Figure 8** "Stack" plots as in Figure 7 for different latitude range for Solar Cycle 22. Horizontal axis is longitude; a sequence of equatorial slices is stacked along the vertical axis with time increasing from bottom to top. Including all of the (left) north polar zone (30° to 70° latitude), (middle) equatorial zone (-20° to +20° latitude), and (right) south polar zone (-70° to -30° latitude).

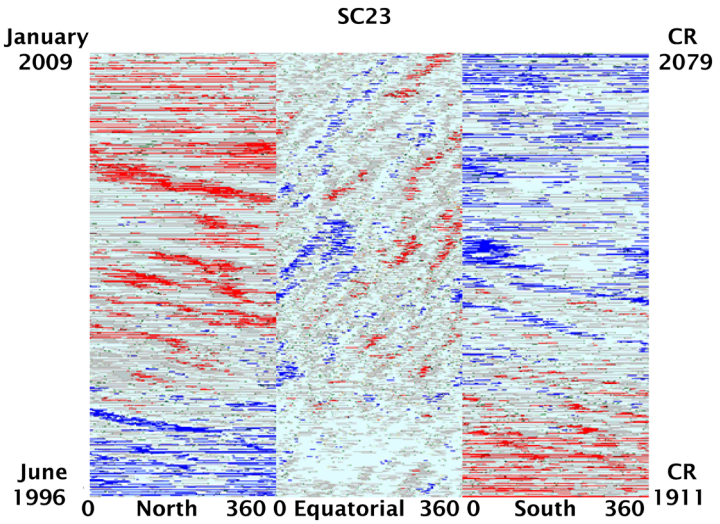


**Figure 9** "Stack" plots as in Figure 7 for different latitude range for Solar Cycle 23. Horizontal axis is longitude; a sequence of equatorial slices is stacked along the vertical axis with time increasing from bottom to top. Including all of the (left) north polar zone (30° to 70° latitude), (middle) equatorial zone (-20° to +20° latitude), and (right) south polar zone (-70° to -30° latitude).

are not uniform as a function of time. This is consistent with Krista, McIntosh, and Leamon (2018), who found that while coronal holes within 10° of the Equator tend to show prograde movement, between 10° and 20° they demonstrate both prograde and retrograde shifts.

These complexities may, at least, partly be a consequence of the fact that coronal holes often span a large range of latitudes. Trans-equatorial holes in particular are stretched into a chevron shape by the differential rotation acting along its vertical extent (see, e.g., Figure 1). In some cases, the trans-equatorial coronal hole breaks into a set of multiple smaller holes that increasingly separate from each other in time. This is illustrated by the 37-rotation coronal hole that can be seen to the left of Figure 6 (blue positive polarity). The stack plot spans latitudes that are asymmetric across the Equator in order to track this particular long-lived coronal hole from the southern to northern hemisphere over its lifetime. As time increases vertically, portions of the coronal hole appear to break off and move retrograde while the rest of the coronal hole continues to move prograde (see also Heinemann et al. (2018) for an analysis of a coronal-hole evolution affected by differential rotation).

It is clear that the centroid latitude of a group of a coronal holes may change with time in a manner that is somewhat ambiguous. Interpretation would require disentangling differential rotation, solar-cycle evolution, coronal-hole lifetime, and coronal-hole visibility. Another challenge arises from the limited information available during solar minimum for analyzing rotation rates vs. latitude due to the fact that there are substantially fewer low-latitude coronal holes at solar minimum than at solar maximum. These effects complicate any attempt to extract a rotation rate for coronal holes vs. latitude from time series such as ours.

However, it is important to consider the sensitivity of the results described in Section 4 to different assumptions of rotation rates. We therefore reran our analysis assuming the photospheric rate as determined by tracking magnetic features (Snodgrass, 1983) (Figure 3, asterisks). In assigning these photospheric rotation rates to the individual coronal holes we chose the rate associated with the latitude of the centroid of that coronal-hole. We tracked coronal holes from rotation to rotation under this assumption by adding the appropriate prograde or retrograde lag to the bounding box used in comparing between Carrington rotations and determining coronal-hole lifetimes.

We found that the results were qualitatively the same as those presented in Section 4, which assumed rigid rotation. Some minor changes arose specific to particular coronal holes. For example, by assuming the photospheric differential rotation rate our tracking method correctly identified the coronal-hole group shown in Figure 6 as having a lifetime of 37 rotations, while the rigid rotation assigned it a value of 33 rotations.

## 6. Conclusions

The McIntosh Archive is a unique resource for studying the evolution of solar magnetic structures over multiple solar cycles. By analyzing the positions and lifetimes of coronal holes over time, we found patterns that vary with the magnetic solar cycle and intertwine with the activity cycle. An important conclusion is how consistent these patterns are from one solar cycle to the next.

The polarity at the poles switches during solar maximum and for a period of approximately six months polar coronal holes are not present, until polar holes of the opposite polarity to those that were there before solar maximum begin to form. Short-lived coronal holes are found at most latitudes in the ascending phase of the solar cycle, and even more so during solar maximum when there are no established polar coronal holes. At solar maximum and the descending phase of the solar cycle, more low-latitude coronal holes are long-lived, appearing closer to the Equator as time passes, in a manner similar to the movement of sunspots and other solar structures.

Regarding lifetimes, we find that the majority of low-latitude coronal holes last less than two rotations, appearing on only one synoptic map. Almost half that last longer than one rotation last for only two rotations. A notable set of low-latitude coronal holes do last for more than ten rotations (in one case we have discussed, almost three years), but these are limited to a handful per solar cycle. Polar coronal holes, on the other hand, tend to last many years, and are particularly dominant at solar minimum. The degree of this dominance seems to vary with solar cycle, however, with Solar Cycles 23 – 24 minimum exhibiting more long-lived low-latitude coronal holes than prior minima (see Figure 2). While it is possible that may in part arise from improved observing capabilities, particular at EUV wavelengths, there is substantial evidence that it is a characteristic associated with the substantially weaker polar magnetic fields associated with that recent solar minimum (de Toma, 2011; Gibson and Zhao, 2012).

We are able to confirm differential rotation of low-latitude coronal holes as seen by previous studies (Navarro-Peralta and Sanchez-Ibarra, 1994; Insley, Moore, and Harrison, 1995; Krista, McIntosh, and Leamon, 2018) – generally prograde near the Equator and retrograde at higher latitudes. We also consider how our analysis is impacted by different assumptions of rigid vs. photospheric differential rotation rates in order to establish that our results are essentially insensitive to these a-priori assumptions about the coronal-hole rotation.

Our findings regarding the evolution and lifetimes of coronal holes are consistent with previous studies, but they are more complete since our observations extend over more than three consecutive solar cycles. In addition, the McA maps trace all important surface magnetic features, including sunspots, plages, filaments, polarity inversion lines, and coronal holes. Thus, we can track how different features evolve in relation to each other over consecutive solar cycles, allowing examination of connected patterns over long time scales. For example, the McA has been used to study high-latitude filament evolution (B. Emery, private communication, 2020). However, we still lack satisfactory knowledge of the solar interior, particularly the deep convection zone. Interior processes ultimately drive the large-scale motions and evolution of the surface features, and these must be accounted for in dynamo models.

Additional future work might include extending the McIntosh Archive of synoptic maps using modern observations. This will require a comparison of He 10830 Å images to EUV 193 Å and 304 Å images for calibration purposes, since good quality and consistent He 10830 Å data are not available after 2015. Finally, the question of how evolution of coronal holes relates to the evolution of sunspots or active regions is an interesting one that we leave for a future analysis (see review by Brown, Canfield, and Pevtsov, 1999).

**Acknowledgements** We thank Beth Schmidt, Patrick McIntosh's daughter, who allowed us to use her father's work, and William Denig who gave us a home for the archive at NCEI. I.M. Hewins and R.H. McFadden thank the HAO for support during their visit and in particular the HAO Coffee and Tea group for all of their assistance. I.M. Hewins, D.F. Webb, R.H. McFadden, B.A. Emery, and T.A. Kuchar were supported by NSF RAPID grant 1540544 and NSF grant 1722727. The National Center for Atmospheric Research is a major facility sponsored by the National Science Foundation under Cooperative Agreement No. 1852977. Finally, we thank the reviewer for their assistance.

**Disclosure of Potential Conflicts of Interest** The authors declare that they have no conflicts of interest.



## References

Altrock, R.C.: 1997, An 'extended solar cycle' as observed in Fe-XIV. *Solar Phys.* **170**, 411. DOI. ADS.

Brown, M.R., Canfield, R.C., Pevtsov, A.A.: 1999, *Magnetic Helicity in Space and Laboratory Plasmas*, *Geophy. Mon. Ser.* **111**, AGU, Washington.
Cranmer, S.R.: 2009, Coronal holes. *Liv. Rev. Solar Phys.* **6**, 2. DOI.
de Toma, G.: 2011, Evolution of coronal holes and implications for high-speed solar wind during the minimum between cycles 23 and 24. *Solar Phys.* **274**, 195. DOI.
Devore, C.R., Sheeley, N.R. Jr., Boris, J.P., Young, T.R.J., Harvey, K.L.: 1985, Simulations of magnetic-flux transport in solar active regions. *Solar Phys.* **42**, 41. DOI.
Gibson, S.E., Zhao, L.: 2012, A porcupine Sun? Implications for the solar wind and Earth. In: Mandrini, C.H., Webb, D.F. (eds.) *Comparative Magnetic Minima: Characterizing Quiet Times in the Sun and Stars*, *IAU Symp.* **286**, Cambridge University Press, Cambridge, 210. DOI. ADS.
Gibson, S.E., de Toma, G., Emery, B., Riley, P., Zhao, L., Elsworth, Y., Leamon, R.J., Lei, J., McIntosh, S., Mewaldt, R.A., Thompson, B.J., Webb, D.: 2011, The whole heliosphere interval in the context of a long and structured solar minimum: An overview from Sun to Earth. *Solar Phys.* **274**, 5. DOI. ADS.
Gibson, S.E., Webb, D., Hewins, I.M., McFadden, R.H., Emery, B.A., Denig, W., McIntosh, P.S.: 2017, Beyond sunspots: Studies using the McIntosh Archive of global solar magnetic field patterns. In: Nandy, D., Valio, A., Petit, P. (eds.) *Living Around Active Stars*, *IAU Symp.* **328**, Cambridge University Press, Cambridge, 93.
Golbeva, E.M., Mordvinov, A.V.: 2017, Rearrangements of open magnetic flux and formation of polar coronal holes in cycle 24. *Solar Phys.* **292**, 175. DOI.
Harvey, K.L., Recely, F.: 2002, Polar coronal holes during cycles 22 and 23. *Solar Phys.* **211**, 31. DOI.
Heinemann, S.G., Temmer, M., Hofmeister, S.J., Veronig, A.M., Vennerstrøm, S.: 2018, Three-phase evolution of a coronal hole. I. 360° remote sensing and in situ observations. *Astrophys. J.* **861**, 151. DOI.
Heinemann, S.G., Jerčić, V., Temmer, M., Hofmeister, S.J., Dumbović, M., Vennerstrom, S., Verbanac, G., Veronig, A.M.: 2020, A statistical study of the long-term evolution of coronal hole properties as observed by SDO. *Astron. Astrophys.* **638**, A68. DOI. ADS.
Hofmeister, S.J., Stefan, J., Veronig, A., Reiss, M.A., Temmer, M., Vennerstrom, S., Vrsnak, B., Heber, B.: 2017, Characteristics of low-latitude coronal holes near the maximum of solar cycle 24. *Astrophys. J.* **835**, 268. DOI.
Hofmeister, S.J., Utz, D., Heinemann, S.G., Veronig, A., Temmer, M.: 2019, Photospheric magnetic structure of coronal holes. *Astrophys. J.* **629**, A22. DOI.
Howe, R.: 2009, Solar interior rotation and its variation. *Liv. Rev. Solar Phys.* **6**, 1. DOI. ADS.
Hundhausen, A.J.: 1972, *Coronal Expansion and Solar*, Springer, Berlin. DOI. ADS.
Hundhausen, A.J., Hansen, R.T., Hansen, S.F.: 1981, Coronal evolution during the sunspot cycle: Coronal holes observed with the Mauna Loa K-coronameters. *J. Geophys. Res.* **86**, 2079. DOI. ADS.
Insley, J.E., Moore, V., Harrison, R.A.: 1995, The differential rotation of the corona as indicated by coronal holes. *Solar Phys.* **160**, 1. DOI. ADS.
Jiang, J., Hathaway, D.H., Cameron, R.H., Solanki, S.K., Gizon, L., Upton, L.: 2014, Magnetic flux transport at the solar surface. *Space Sci. Rev.* **186**, 491.
Karak, B.B., Jiang, J., Miesch, M.S., Charbonneau, P., Choudhuri, A.R.: 2014, Flux transport dynamos: From kinematics to dynamics. *Space Sci. Rev.* **186**, 561.
Krieger, A.S., Timothy, A.F., Roelof, E.C.: 1973, A coronal hole and its identification as the source of a high velocity solar wind stream. *Solar Phys.* **29**, 505. DOI.
Krista, L.D., McIntosh, S.W., Leamon, R.J.: 2018, The longitudinal evolution of equatorial coronal holes. *Astron. J.* **155**, 153. DOI. ADS.
Lockyer, W.J.S.: 1931, On the relationship between solar prominences and the forms of the corona. *Mon. Not. Roy. Astron. Soc.* **91**, 797. DOI. ADS.
Lowder, C., Qiu, J., Leamon, R.: 2017, Coronal holes and open magnetic flux over cycles 23 and 24. *Solar Phys.* **292**, 18. DOI. ADS.
Mazumder, R., Bhowmik, P., Nandy, D.: 2018, The association of filaments, polarity inversion lines, and coronal hole properties with the sunspot cycle: An analysis of the McIntosh database. *Astrophys. J.* **868**, 52. DOI. ADS.
McIntosh, P.S.: 1979, *Annotated Atlas of H-Alpha Synoptic Charts for Solar Cycle 20 (1964-1974) Carrington Solar Rotations 1487-1616*, U.S. Dept. Commerce, Boulder, ADS.
McIntosh, S.W., Leamon, R.J., Krista, L.D., Title, A.M., Hudson, H.S., Riley, P., Harder, J.W., Kopp, G., Snow, M., Woods, T.N., Kasper, J.C., Stevens, M.L., Ulrich, R.K.: 2015, The solar magnetic activity band interaction and instabilities that shape quasi-periodic variability. *Nat. Commun.* **6**, 6491. DOI. ADS.
Navarro-Peralta, P., Sanchez-Ibarra, A.: 1994, An observational study of coronal hole rotation over the sunspot cycle. *Solar Phys.* **153**, 169. DOI. ADS.
Snodgrass, H.B.: 1983, Magnetic rotation of the solar photosphere. *Astrophys. J.* **270**, 288. DOI. ADS.
Waldmeier, M.: 1957, *Die Sonnenkorona*, Birckhäuser, Basel.

Waldmeier, M.: 1981, Cyclic variations of the polar coronal hole. *Solar Phys.* **70**, 251. DOI. ADS.
Wang, Y.-M., Sheeley, N.R. Jr.: 1990, Solar wind speed and coronal flux-tube expansion. *Astrophys. J.* **355**, 726.
Webb, F.D., Davis, J.M., McIntosh, P.S.: 1984, Observations of the reappearance of polar coronal holes and the reversal of the polar magnetic field. *Solar Phys.* **92**, 109. DOI.
Webb, D.F., Gibson, S.E., Hewins, I.M., McFadden, R.H., Emery, B.A., Malanushenko, A., Kuchar, T.A.: 2018, Global solar magnetic field evolution over 4 solar cycles: Use of the McIntosh archive. *Front. Astron. Space Sci.* **5**, 23. DOI. ADS.
Wilcox, J.M.: 1968, The interplanetary magnetic field. Solar origin and terrestrial effects. *Space Sci. Rev.* **8**, 258. DOI. ADS.
Zhang, Y., Wang, J., Attrill, G.D.R., Harra, L.K., Yang, Z., He, X.: 2007, Coronal magnetic connectivity and EUV dimmings. *Solar Phys.* **241**, 329. DOI. ADS.
Zirker, J.B.: 1977, Coronal holes - an overview. In: Zirker, J.B. (ed.) *Coronal Holes and High Speed Wind Streams*, Colorado University Press, Boulder, 1. ADS.